Supporting Information for "Detecting climate signals using explainable AI with single-forcing large ensembles"

Zachary M. Labe[1]and Elizabeth A. Barnes[1]

[1]Department of Atmospheric Science, Colorado State University, Fort Collins, CO, USA

Contents of this file

1. Table S.1 to S.2
2. Figures S.1 to S.6
3. References

Corresponding author: Zachary M. Labe (zmlabe@rams.colostate.edu)

Table S.1. Description of climate model data sets used for the primary analysis in this study.

Name	Forcing	Years	# Members	Reference
ALL	Historical (to 2005), RCP 8.5	1920–2080	20	CESM-LE - Kay et al. (2015)
AER+	ALL, but fixed greenhouse gases to 1920 levels	1920–2080	20	XGHG - Deser et al. (2020)
GHG+	ALL, but fixed industrial aerosols to 1920 levels	1920–2080	20	XAER - Deser et al. (2020)

Table S.2. Description of observational data sets used for the primary analysis in this study.

Name	Data Set	Years	Reference
20CRv3	NOAA-CIRES-DOE 20th Century Reanalysis V3	1920–2015	Slivinski et al. (2019)

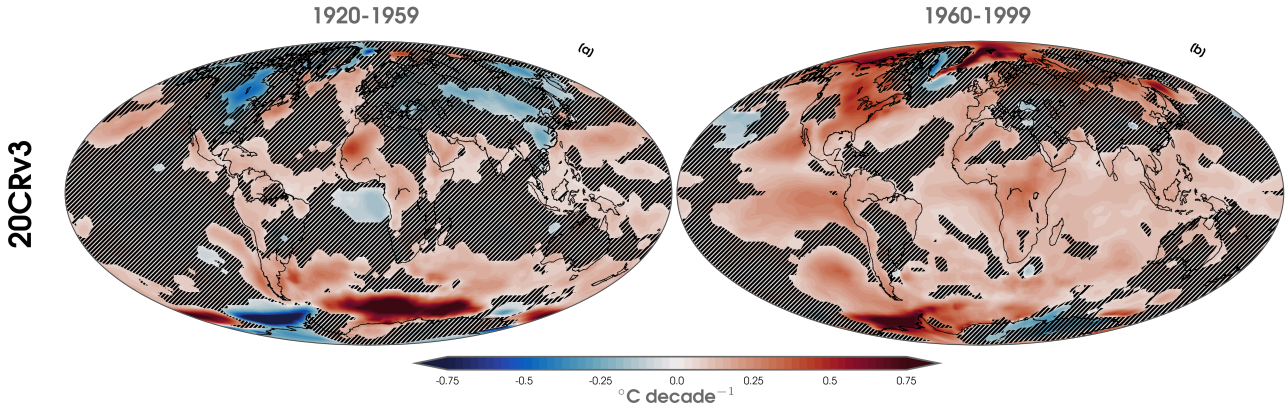

Figure S.1. Annual linear least squares trends of 2-m temperature (°C per decade) over 1920 to 1959 (a) and 1960 to 1999 (b) using 20CRv3 reanalysis (observations). Statistically significant trends are shown with shaded contours at the 95% confidence level following the Mann-Kendall (MK) test (Mann, 1945; Bevan & Kendall, 1971). Insignificant trends are masked out using black hatch marks.

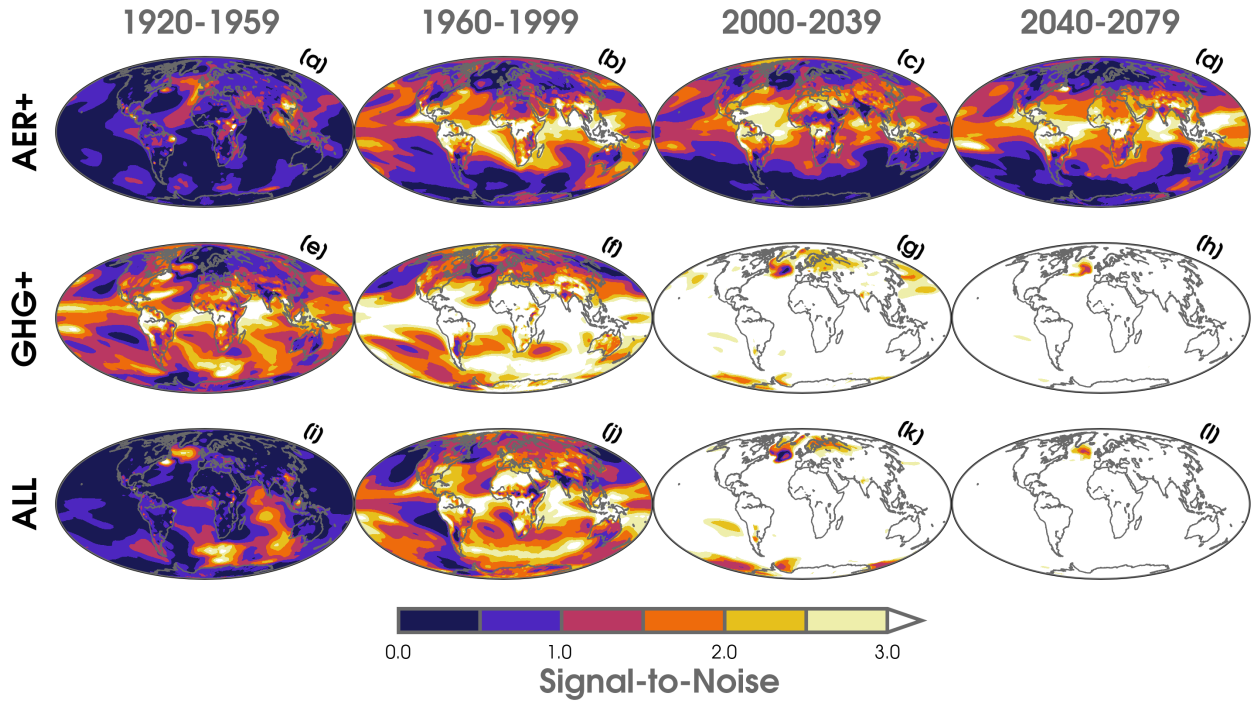

Figure S.2. Signal-to-noise ratio (SNR) maps of annual mean 2-m temperature over 1920 to 1959 (a,e,i), 1960 to 1999 (b,f,j), 2000 to 2039 (c,g,k), and 2040 to 2079 (d,h,l) for three climate model simulations (AER+; a-d, GHG+; e-h, ALL; i-l). SNR is calculated here as the absolute value of the ensemble mean trend (forced response) normalized by the standard deviation of trends across individual ensemble members (internal variability) for each 40 year period.

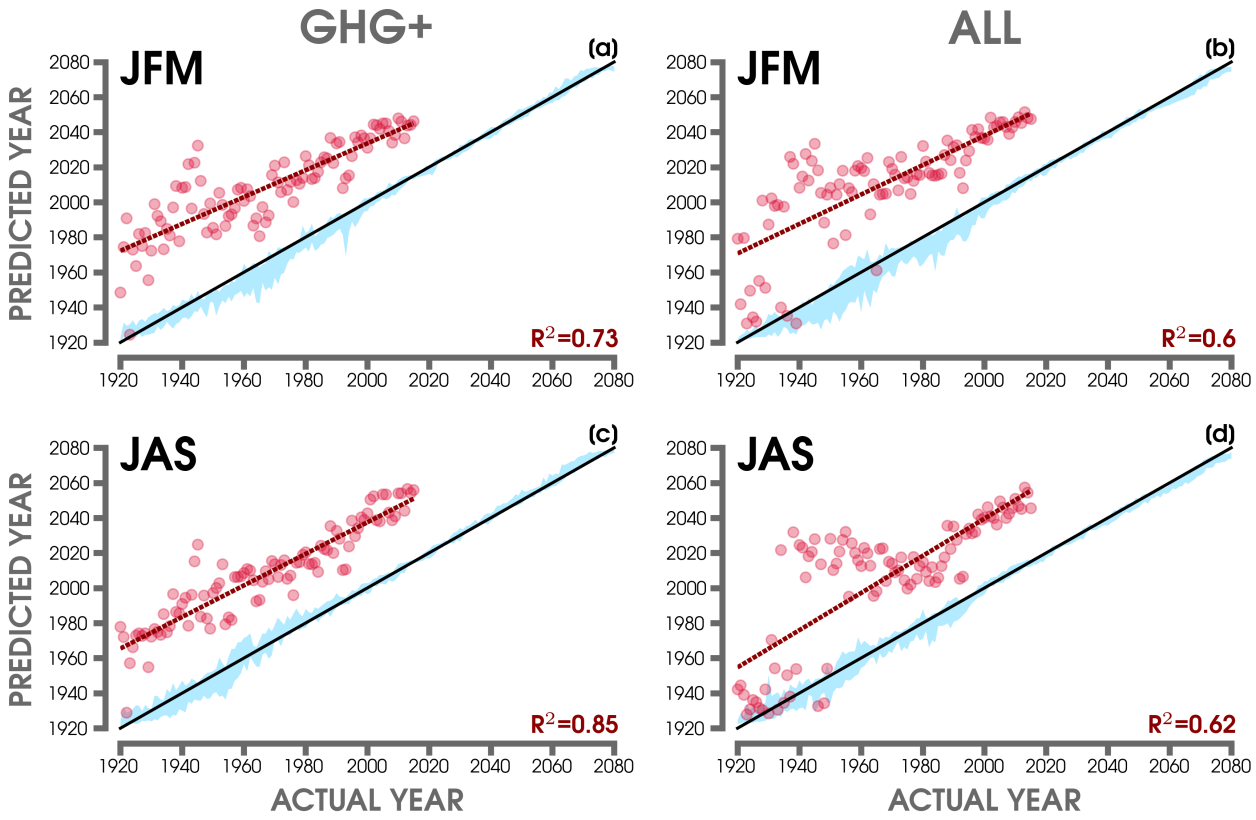

Figure S.3. (a) ANN predictions of the year (y-axis) compared to the actual year (x-axis) by models trained on global maps of 2-m temperature in GHG+ (a,c) and ALL (b,d) during January-February-March (JFM; a,b) and July-August-September (JAS; c,d). The blue shading highlights the 5th-95th percentiles of predictions from the combined training and testing large ensemble data. The red points show the predictions using 20CRv3 observations. The red dashed line shows the linear least squares fit through the predicted observations in each model, and its R^2 is shown in the lower right-hand corner. The 1:1 line is overlaid in black.

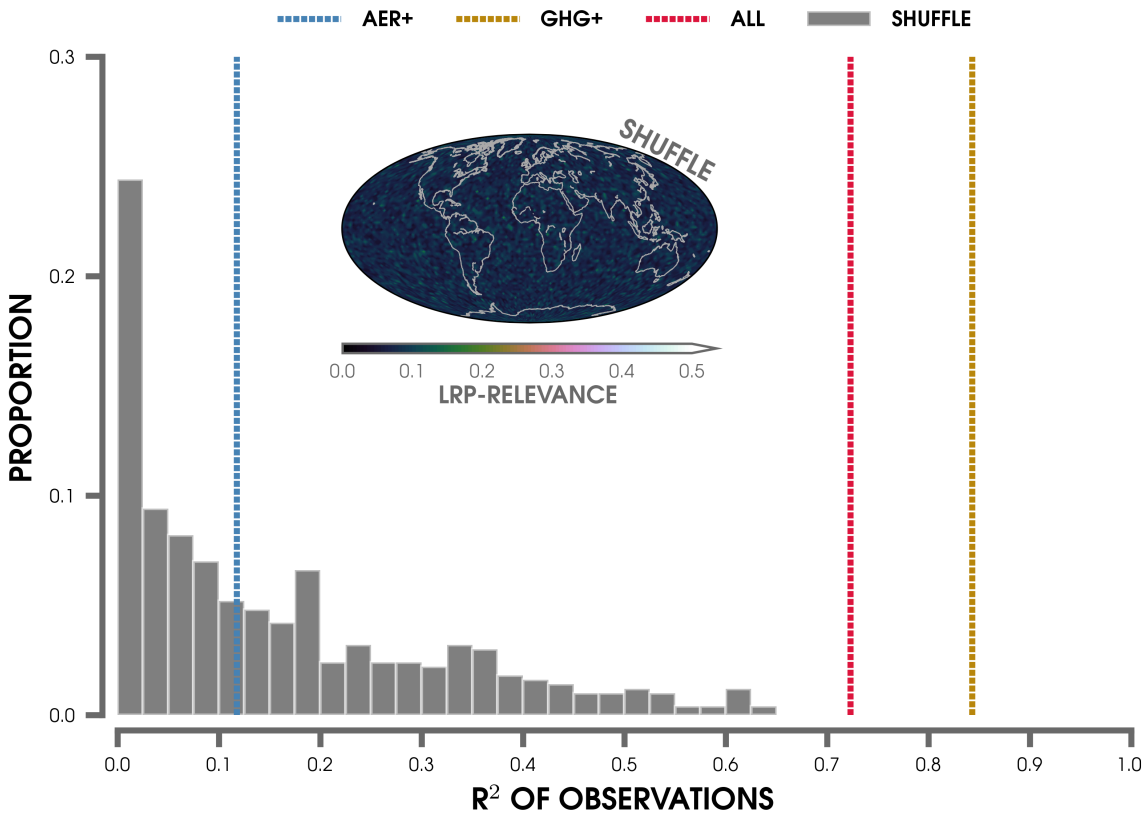

Figure S.4. Histogram of the possible R^2 values from the linear fit of predicted 20CRv3 observations after randomly shuffling the individual ensemble members and years of ALL input data to obtain 500 iterations of the ANN. The median R^2 values of the possible predictions of observations using the ANNs for AER+ (blue), GHG+ (brown), and ALL (red) are overlaid by the dashed vertical lines (as in Figure 3). An example (single iteration) of a LRP heatmap is also shown based on the ANN of shuffled ALL input data (averaged from 1920 to 2080).

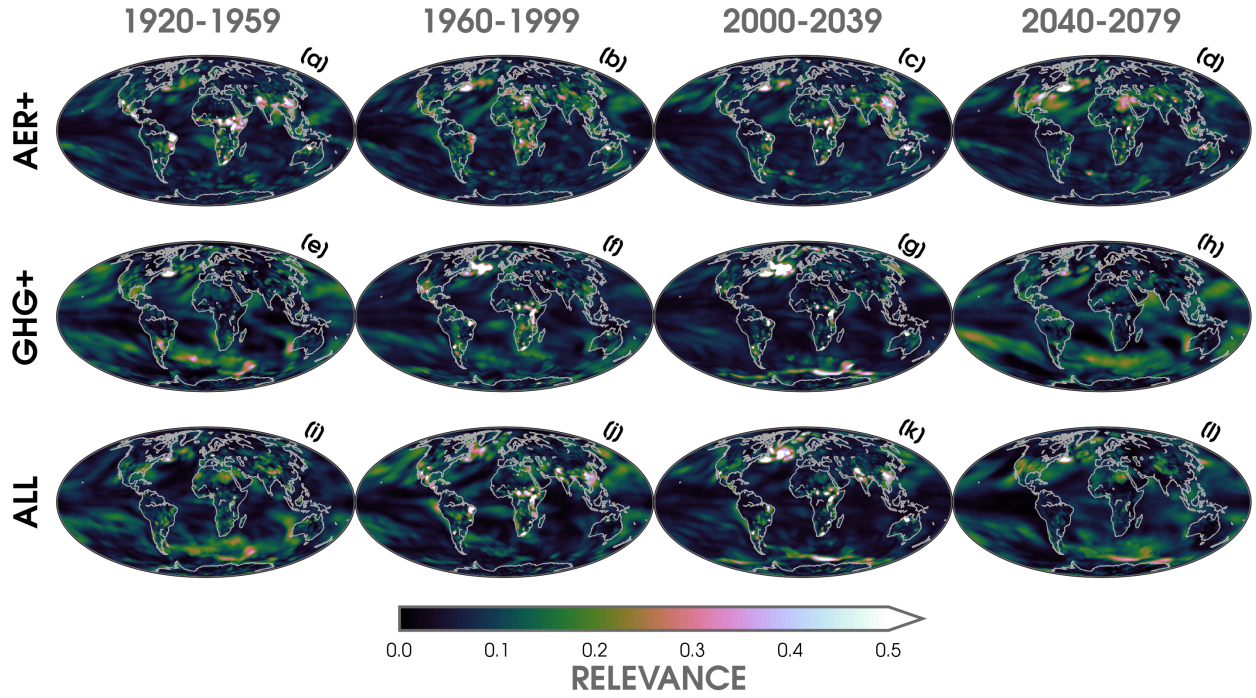

Figure S.5. LRP composite heatmaps averaged over 1920 to 1959 (a,e,i), 1960 to 1999 (b,f,j), 2000 to 2039 (c,g,k), and 2040 to 2079 (d,h,l) for the three large ensemble experiments (AER+; a-d, GHG+; e-h, ALL; i-l). Higher LRP values indicate greater relevance for the ANN's prediction.

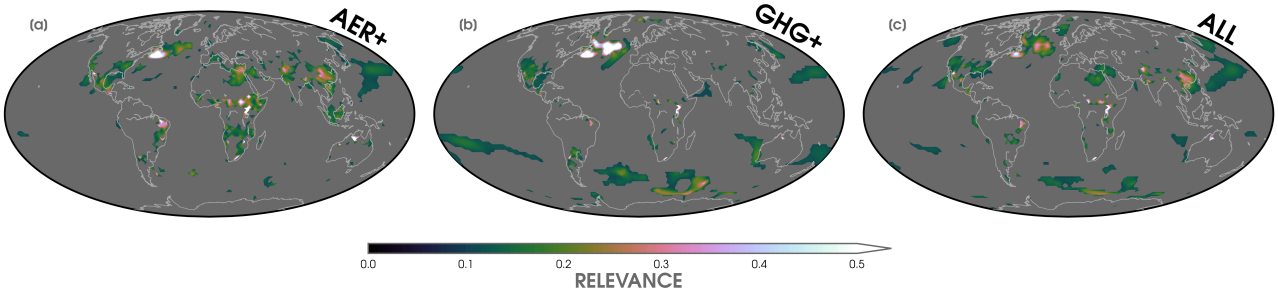

Figure S.6. (a) Composite of LRP heatmaps over 1960 to 2039 for inputs of annual 2-m temperature (global) maps from AER+. (b) Same as (a) but for GHG+. (c) Same as (a) but for ALL. LRP composites are generated by averaging across 100 possible ANN iterations by using different combinations of training and testing data for each large ensemble. Relevance values less than the 95th percentile threshold have been masked out (gray shading). Higher LRP values indicate greater relevance for the ANN's prediction.

References

Bevan, J. M., & Kendall, M. G. (1971). Rank Correlation Methods. *The Statistician*. doi: 10.2307/2986801

Deser, C., Phillips, A. S., Simpson, I. R., Rosenbloom, N., Coleman, D., Lehner, F., ... Stevenson, S. (2020, sep). Isolating the Evolving Contributions of Anthropogenic Aerosols and Greenhouse Gases: A New CESM1 Large Ensemble Community Resource. *Journal of Climate*, *33*(18), 7835–7858. Retrieved from `https://doi.org/10.1175/JCLI-D-20-` doi: 10.1175/JCLI-D-20

Kay, J. E., Deser, C., Phillips, A., Mai, A., Hannay, C., Strand, G., ... Vertenstein, M. (2015, aug). The Community Earth System Model (CESM) Large Ensemble Project: A Community Resource for Studying Climate Change in the Presence of Internal Climate Variability. *Bulletin of the American Meteorological Society*, *96*(8), 1333–1349. Retrieved from `http://journals.ametsoc.org/doi/10.1175/BAMS-D-13-00255.1` doi: 10.1175/BAMS-D-13-00255.1

Mann, H. B. (1945). Nonparametric Tests Against Trend. *Econometrica*. doi: 10.2307/1907187

Slivinski, L. C., Compo, G. P., Whitaker, J. S., Sardeshmukh, P. D., Giese, B. S., McColl, C., ... Wyszyński, P. (2019, oct). Towards a more reliable historical reanalysis: Improvements for version 3 of the Twentieth Century Reanalysis system. *Quarterly Journal of the Royal Meteorological Society*, *145*(724), 2876–2908. Retrieved from `https://onlinelibrary.wiley.com/doi/abs/10.1002/qj.3598` doi: 10.1002/qj.3598